Position sensorless field-oriented control of BLDC motor for EV applications

Vinay Kumar Awaar[1*]*, Anjali* Nagilla[1], *Sravani* Bannuru[1], *Suchitha* Veeramaneni[1], *Prasanthi* Veerla[1], *A. Hussien* Abbas[2]

[1]Gokaraju Rangaraju Institute of Engineering and Technology, Telangana, India.
[2]Computer Technical Engineering Department, College of Technical Engineering, The Islamic University, Najaf, Iraq

Abstract. A brushless DC motor (known as BLDC) is a permanent magnet synchronous electric motor which is driven by direct current (DC) electricity, and it accomplishes an electronically controlled commutation system instead of a mechanical commutation system. Major of the BLDC applications are based on speed control like motors used in electric vehicles, washing machines, air conditioners, etc. For the speed regulation of BLDC, TMS320F2837xD and TMS320F28069M microcontrollers are used, which belong to the C2000 family. These microcontrollers are used to increase efficiency by reducing the system components and enabling a cost-effective design of intelligent controllers for three-phase motors. With these devices, digital vector control algorithms like field-oriented control (FOC) may be implemented with much more precision. By computing a dynamic model of the motor, the FOC algorithm maintains efficiency across a wide speed range and considers torque variations with transient phases. The ideas include strategies to get rid of the phase current sensors and switch to sensorless speed control with an observer. The proposed model simulations can be achieved using MATLAB simulation tools, Graphical User Interface (GUI) application and Code Composer Studio (CCS).

1 Introduction

Brushless Dc motors are used widely for industrial applications. To understand the working of the Brushless, we need to know the workflow of the brushed DC motor. As the name describes it contains brushes and takes DC power as input. A brushed DC motor contains a spinning armature on the inside and permanent magnets on the outside of its structure. The rotating part of the armature having the electromagnet is called the rotor. And a stator is

---

* Corresponding author: vinaykumaar.a@gmail.com

termed the stationary part of the permanent magnets on the outside. When an electric current is passed to the armature the motor spins at 180 degrees. To move beyond which is around 360° the poles of the electromagnet must flip. This is accomplished, when the rotor spins, and the brushes come in contact with the stator, flipping the magnetic field and making the rotor move up to full (360°). A similar process is followed in the brushless too. The difference is, by the elimination of brushes and making the motion control flow more precise by the use of computer-controlled electric current, the efficiency is increased. Here, the permanent magnets are at the rotor and electromagnets on the stator. A brushless DC motor [1] is flipped inside out, which makes the size compact by eliminating brushes to flip the electromagnetic field. The computers are used for the charging of the electromagnets in the stator for the purpose of full rotation (360°). Due to their lightweight, quiet nature, ease of maintenance, reliability, and compact size, brushless DC motors are more efficient [2]. The speed of the motor can be controlled using sensors or using sensorless[3]. The only difference is the efficiency, the speed control method which uses senseless i.e. using observers increases the efficiency of the speed control method more than the method which uses sensors to get the position of the motor. The aim of the project is to control the speed of the BLDC motor using the controller LAUNCHXL TMS320F2837xD [4] aligning with a BOOSTXL-DRV8305 and LAUNCHXL TMS320F28069M aligning with a - BOOSTXL DRV8301 [5] inverter and interfacing with software models developed in MATLAB and GUI. The speed of the controller is controlled using Field oriented control (FOC) algorithm[6]. The algorithm is implemented in the blocks of software models developed.

2   Speed control methods of BLDC motor

2.1   Trapezoidal control

Trapezoidal control also known as 6-step commutation contains a three-phase H Bridge Inverter creating 6 flow vectors to cause 60° rotation corresponding to the next position [7]. Since the rotor position defines the direction of the current, hall sensors are placed to obtain the speed and position of the rotor and provide rotor position feedback to the controller and speed to the microcontroller to drive the motor. The current is controlled by driving one pair at a time and the third motor terminal is electrically disconnected. When the Rotor spins, the Hall sensors get activated and they generate a repeating signal but a shifted one, and hence six independent hall states are observed based on rotor position as shown in figure 1.
Though this method is easy for commutation and has fewer switching losses some of which disadvantages include less efficiency and more noise.
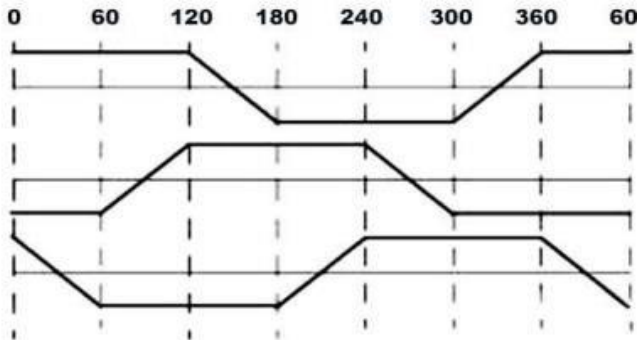

Figure 1. 6-step commutation

2.2   Sinusoidal control

This control is also called 180° commutation and is not like trapezoidal control where 100% On or 100% Off states are observed. To overcome the disadvantages of trapezoidal control here in the sine control algorithm we apply a smoother voltage waveform by giving PWM to phases. This control has more resolution and can be achieved with or without sensors. This control causes low noise than trapezoidal control and is easy than FOC, but it has high switching losses, low maximum four speed, and does not have a great load performance.

2.3   Field-oriented control

FOC also called vector control is an advanced sine control [8] that helps achieve better dynamic performance and is complex compared to the other two. This method uses a mathematical transformation to decouple torque and magnetizing flux [9]. The main aim is that the windings are driven so as to keep the rotor magnetic field orthogonal to the stator magnetic field. This control is explained in detail in the block diagram section and the attached figure 2 represents the algorithm of this control.
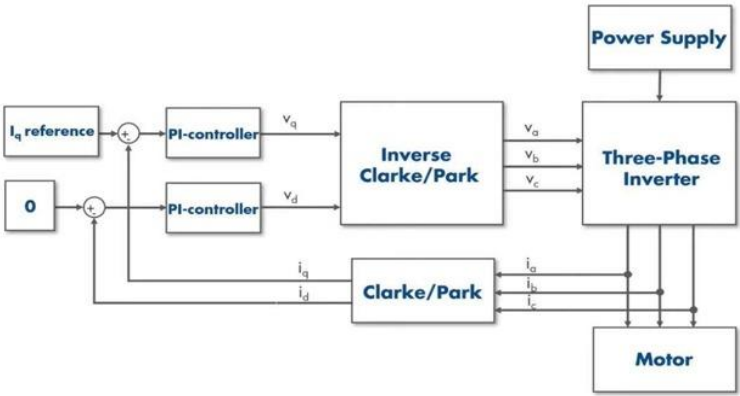

Figure 2. FOC algorithm

3   Position sensorless FOC

3.1   Introduction

A BLDC is a type of synchronous motor and in such a machine, the torque produced is equal to the cross product of stator and rotor magnetic fields ($T_{syn} = B_{stator} \times B_{rotor}$) in order to achieve maximum torque conditions the angle between these two should be 90°. By doing so we reduce torque ripple and observe a better dynamic response. The stator current vector is defined as the sum of instantaneous currents in the stator phases, so by varying the phase currents we can compute for stator field vector based on rotor position.

3.2   Sensorless speed control of the BLDC motor using FOC

The fixed DC is given to the voltage source inverter [10] for electric communication and given to the BLDC motor which is shown in figure 3. We first measure any two of the phases. As we know the sum of phase currents is zero, measuring the third phase current is not required. These currents which are in 3-axis stationary reference frame are converted to a 2-

axis orthogonal stationary reference frame with the help of the Clarke transform. i.e., I_a, I_b, I_c → i_α, i_β and in turn given to Park transform to convert to 2-axis rotating reference frame i_d, i_q. I_d representing the direct axis current is parallel to the rotor magnetic field and I_q which is the quadrature axis current is perpendicular to the rotor magnetic field. These two currents are in DC and are the components of the stator magnetic field. For optimal torque, we force the i_d to zero and maximize i_q so as to obtain orthogonality between stator and rotor magnetic fields.
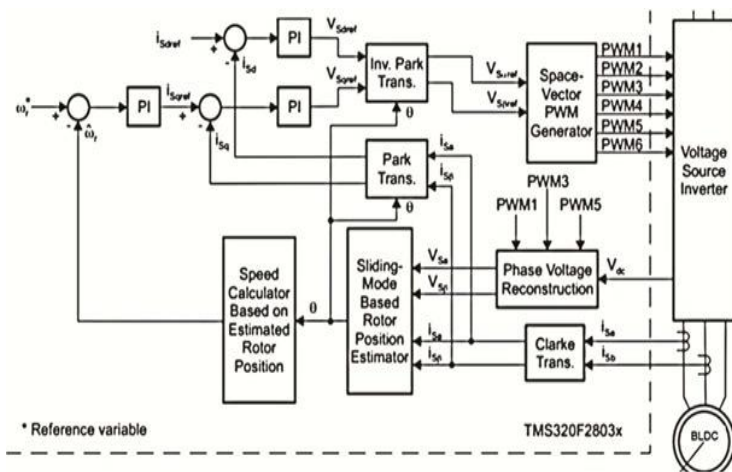

Figure 3. Block diagram of sensorless speed control of BLDC motor using FOC

The id reference is set to zero and id from the park transform is compared and the error signal is given to the PI flux controller. Whereas I_q reference is obtained from the speed feedback loop and I_q from park transform is compared and the error signal is given to the PI torque controller hence obtaining V_d reference and V_q reference. These two signals are given to inverse park and Clarke transform to convert back to AC 3-axis stationary reference frame and the gate pulses are provided to the inverter. We can replace the inverse Clarke transform with a Space vector PWM generator to provide pulses. In the absence of hall sensors, we use SMO or Flux observer. In this block diagram, the SMO takes 4 inputs i_α, i_β, V_α, V_β and internally calculated back EMF to know the rotor position θ. The feedback speed is calculated as ω feedback= dθ /dt with the help of the Speed calculator [11]. The error speed is given to the PI speed controller to obtain an I_q reference. The PI controllers ensure that the error is reduced.

4   Hardware implementation

For the implementation of the hardware setup, model mentioned in [12] is used. The model has two setup models i.e. target model and host model. The host model takes the input from the user in which speed the motor has to run(reference speed) and the target model has four blocks namely serial receiver, speed control, current control, inverter and motor. The serial

receiver gets the rotor position which in turn calculates the speed by the formula $d\theta/dt$ and this speed is given as an input to the speed control block. The speed control block compares the actual speed with the reference speed and generates an equivalent i_{dq_ref} as explained in the section 3 , the current is given as an input to the current control block. FOC algorithm is implemented in the current control block and generates duty cycles. These generated duty cycles are given to the inverter so that the voltage is changed thus the speed of the motor is controlled.
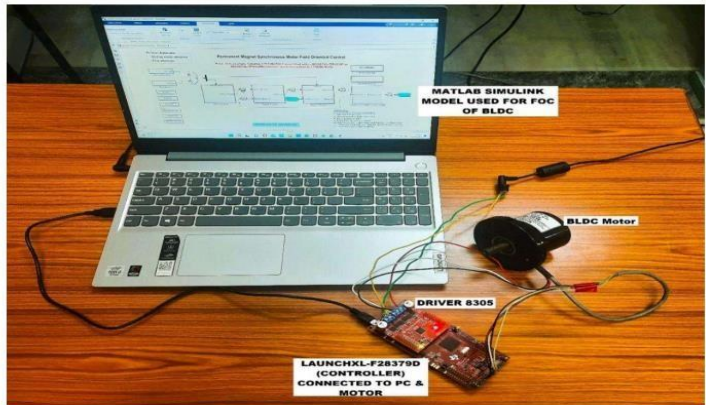
Figure 4. Hardware setup of BLDC motor connected drive.

The hardware setup containing components such as controller board LAUNCHXL-F28379D, inverter board BOOSTXL-DRV8305, BLDC motor, 24V DC supply, and a laptop for the software and hardware interface is shown in figure 4. The hardware connections are as follows. The inverter board is connected to the controller board such that J1, J2 of BOOSTXL-DRV8305 (inverter board) and J1, J2 OF LAUNCHXL-F28379D (controller board) are aligned.

The three phases of the BLDC motor are connected to the BOOSTXL-DRV8305 inverter board's MOA, MOB, and MOC. DC power supply (24V) is given to the inverter board's PVDD and GND. Sensors are connected to the controller board. To control the speed of the BLDC, motor the hardware has to interface with the simulation model for which USB cable is used to interface the alignment connection of inverter BOOSTXL and controller LAUNCHXL with the simulation model designed in MATLAB.

The speed of the motor is controlled by interfacing the hardware setup and the software simulation model which is done by USB cable. Once the connections and interface are done the target model is built and deployed. The code is generated in CCS and is deployed in the controller LAUNCHXL upon successful compilation. Once the code is deployed, we will go to the Host model and select the COM port in the serial setup and give a reference speed and run the model [12]. It is observed that the motor runs at the reference speed given in the host model.

The speed of the motor can be controlled by giving a reference speed in the host model within the rating of the motor. By selecting the radio buttons in debug signals, the scope shows the

respective graph for the respective speed. The motor can be analysed by giving different reference speed and comparing the graphs which is done and mentioned in this paper.

4.1 Evaluation of parameters of BLDC motor at various speeds

The hardware results of different graphs at respective speed that is 500rpm are shown below.
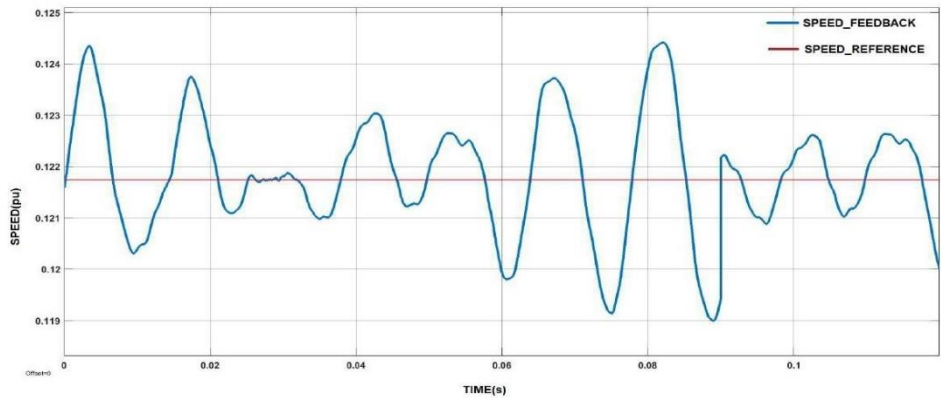

Figure 5. speed_reference and speed_feedback

Speed_reference and speed_feedback with respect to time for the speed 500rpm is shown in figure 5. The time (sec) is taken on the x-axis and speed (per unit value) is taken on the y-axis. The red line in the figure indicates speed_reference. It is observed that the speed_reference is constant at the speed given as reference in the host model. The blue line indicates speed_feedback and the magnitude of the feedback depends on the ripples and rotor position.
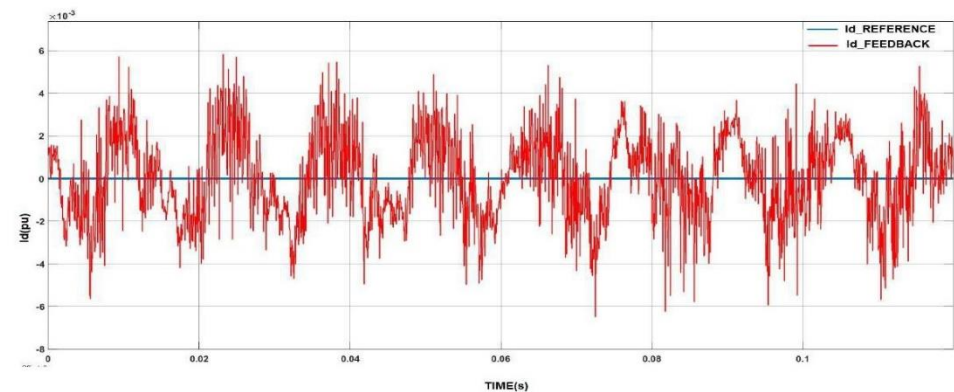

Figure 6. I_d_reference and I_d_feedback

I_d_reference and I_d_feedback with respect to time for the speed 500rpm is shown in figure 6. The time (sec) is taken on the x-axis and the direct axis current Id (per unit value) is taken on the y-axis. The blue line in the figure indicates I_d_reference. The value of I_d_reference is set to zero as already discussed. The red line indicates I_d_feedback.
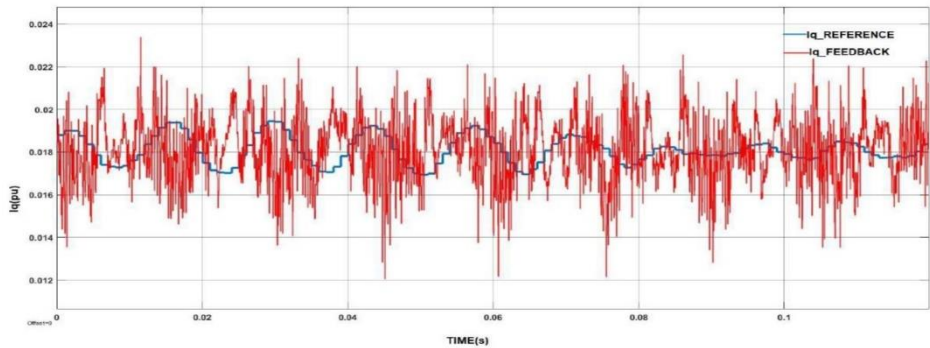

Figure 7. I_q_reference and I_q_feedback

I_q_reference and I_q_feedback with respect to time for the speed 500rpm is shown in figure 7. The time (sec) is taken on the x-axis and the quadrature axis current I_q(per unit value) is taken on the y-axis. The blue line in the figure indicates I_q_reference. The red line indicates I_q_feedback.
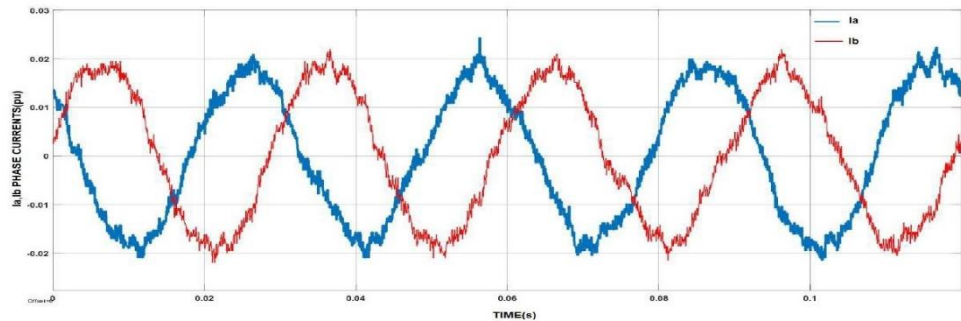

Figure 8. I_a and I_b

Phase current I_a and phase current I_b with respect to time for the speed 500rpm is shown in figure 8. The time (sec) is taken on the x-axis and phase currents (per unit value) are taken on the y-axis. The blue line in the figure indicates phase current Ia. The red line indicates the phase current Ib. It is observed that the magnitude of the phase currents changes when there is an external pressure applied to the motor.
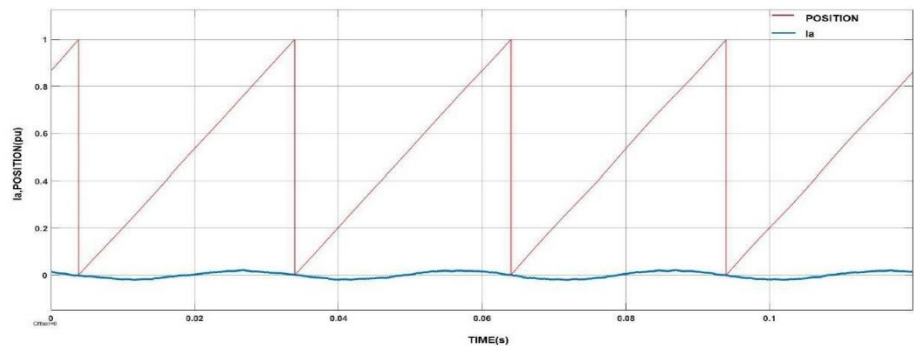
Figure 9. I_a and rotor position

Phase current I_a and rotor position with respect to time for the speed 500rpm is shown in figure 9. The time (sec) is taken on the x-axis and I_a and rotor position (per unit value) are taken on the y-axis. The blue line in the figure indicates the phase current Ia. The red line indicates the rotor position of the motor. It is observed that the width of the saw tooth representing the rotor position of the motor decreases as the speed increases. Similarly, the graphs at different speeds up to 2600 have been taken.

4.2 Analysis of BLDC motor parameters at various speeds

The below are the analysis graphs drawn from the values of the rotor position and currents taken at different speeds.
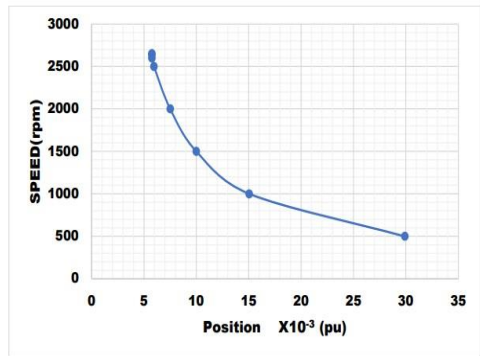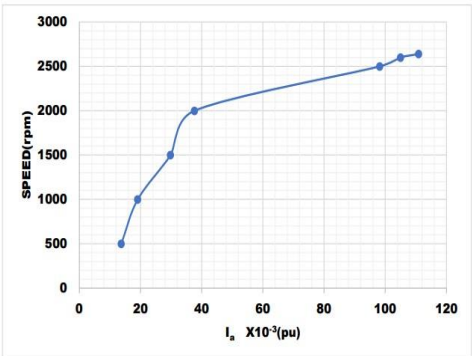

Figure 10. Speed and rotor position
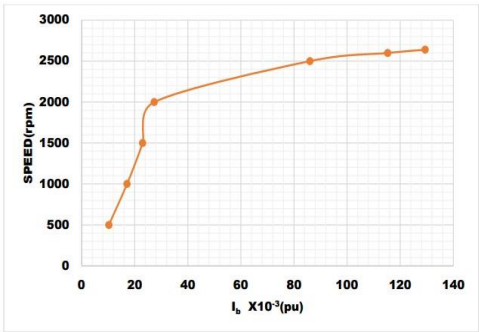
Figure 11. Speed and I_a

Figure 12. Speed and I_b

As the speed increases the rotor position decreases which is shown in figure 10 where the rotor position is taken on the x-axis and speed is taken on the y-axis. As the speed increases the phase current I_a also increases which is shown in figure 11 where phase current I_a is taken on the x-axis and speed is taken on the y-axis. As the speed increases the phase current I_b also increases which is shown in figure 12 where phase current I_b is taken on the x-axis and speed is taken on the y-axis.
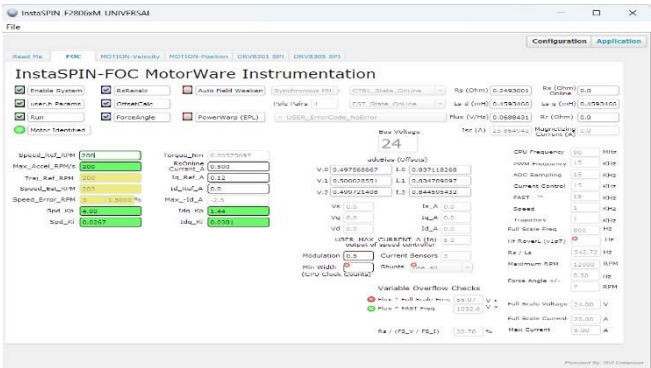
4.3 Parameters estimation with GUI application
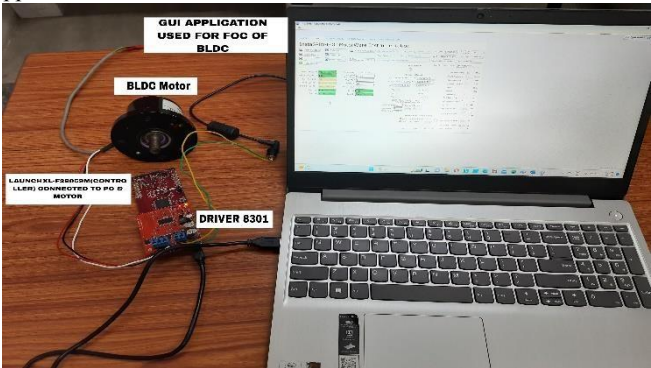

Figure 13. GUI application

Figure 14. Hardware interfacing with GUI

 The GUI application which is shown in figure 13 consists of configuration and application. Program files such as 5c.out, 5e.out, 6a.out, 10b.out indicating sensorless velocity control [13] are taken directly from Code Composer Studio (CCS) and save one of them in GUI composer webapps by renaming it as appprogram.out. Then the hardware is connected to the computer using USB cable which is shown in Figure 14. GUI composer automatically reads the appprogram.out file and directs to the application page. Then open FOC in GUI, select enable system and run. In the reference speed block, change the speeds as per the requirement. Here, the speed has been increased from 100 to 2600 and changes in the parameters such as torque, current, flux which are displayed on the screen have been noted.

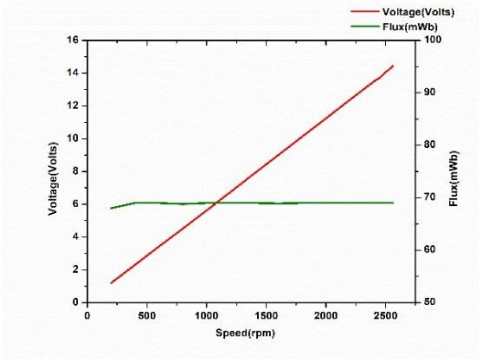The graphs are plotted below using the values noted from the GUI software at no load condition.

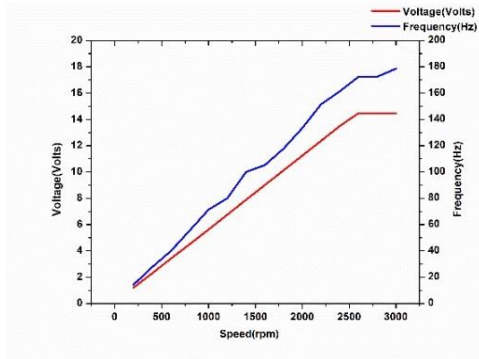

Figure 15. Speed, voltage and flux

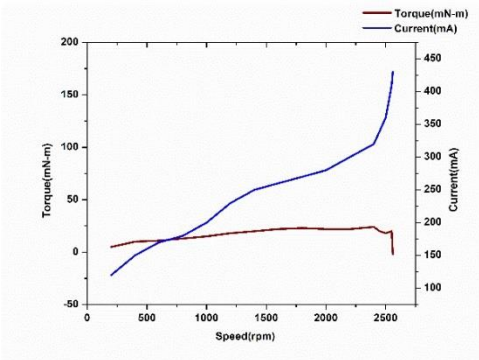**Figure 16.** Speed, voltage and frequency

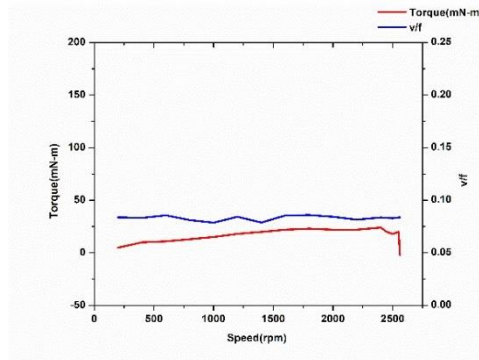
Figure 17. Speed, torque and current

Figure 18. Speed, torque and v/f

The graph which is shown in figure 15 states that with the increase in the speed, voltage increases linearly from 1v at 200rpm to 15v at 2500rpm and remains constant further, the flux increases slowly from 68mWb at the start that is 300rpm and reaches approximately 70mWb and remains constant from 500rpm. The graph which is shown in figure 16 states that with the increase in the speed, voltage increases linearly from 1v at 200rpm to 15v at 2500rpm and remains constant further, frequency raises from 10Hz at speed 200rpm and increases gradually with small fluctuations. The graph which is shown in figure 17 states that with the increase in the speed, torque increases gradually from almost 0 to 10 at speed 200rpm, increases with only slight change and falls to approximately 15mN-m and decreases with a sharp downfall of 5mN-m at 2500rpm, current increases from around 120mA at speed

200rpm and increases gradually up to 330mA and increases with a sharp rise till 440mA at speed 2400rpm. The graph which is shown in figure 18 states that with the increase in the speed, torque increases gradually from almost 0 to 10 at speed 200rpm, increases with only slight change and reaches to approximately 15mN-m and decreases with a sharp downfall of -5mN-m at 2500rpm, v/f remains almost constant of 0.07v/Hz with small fluctuations from speed 200rpm.

5   Conclusion

This paper has presented the model in which Field oriented control is used to control the speed of the BLDC where Torque and Speed may be regulated independently. Two currents responsible for Torque and Field are resolved and maintained separately. The proposed methodology was created and proved to be more efficient than the existing method in terms of control strategies. The graphs of different parameters like speed, direct axis current, quadrature current, phase currents, and position of the motor at the respective speed reference mentioned in the Host model are included. The graphs of parameters such as torque, speed, flux, frequency, voltage, current and v/f are also included. By taking the values of the parameters from the graphs an analysis report of parameters with respect to speed is also presented.

References

1.   Design and implementation of brushless dc motor drive and control system, 2017 7th IEEE International Conference on Control System, Computing and Engineering (IWIEE 2017), Huazhang WANG*, Chengdu, 610041, China, 28–30 December (2017)

2.   Awaar Vinay Kumar, Praveen Jugge, S. Tara Kalyani, and Mohsen Eskandari, Dynamic voltage restorer–A custom power device for power quality improvement in electrical distribution systems. In Power Quality: Infrastructures and Control, pp. **97-116**. Singapore: Springer Nature Singapore, (2023)

3.   J.C. Gamazo-Real, E. Vázquez-Sánchez, J. Gómez-Gil, Position and speed control of brushless dc motors using sensorless techniques and application trends, Sensors. **10**(7):6901-6947 (2010)

4.   Awaar V. K, P. Jugge, & Tara Kalyani, Validation of control platform using TMS320F28027F for dynamic voltage restorer to improve power quality, S. Journal of Control Automation and Electrical Systems **30**, no.4 (2019): pp 601-610

5.   V. K. Awaar, P. Jugge and Tara Kalyani S, Field test of cost-effective voltage source inverter for driving an induction Motor, 2015 Annual IEEE India Conference (INDICON), New Delhi, (2015), ISBN: 978-1-4673-7399-9, pp.**1-6**

6.   Field oriented controller for brushless dc motors, IA40LT Tarmo Prillop 103762IASB (2017)

7.   A.A Mousmi and Y. El Houm, Trapezoidal control of brushless dc motor based on DSP F28335, International Conference on Wireless Technologies, Embedded and Intelligent Systems (WITS) (2017), pp. **1-5**

8.   D. Rau, J. Rodina, P. Hubinsky, Sensorless field-oriented control of BLDC motors for MAVS, Transactions on Electrical Engineering (2015)

9.   Kellen D. Carey, B.S, Hybrid sensorless field oriented and direct torque control for variable speed brushless dc motors, Milwaukee, Wisconsin May (2018)

10. Venu Gopal Mangali, Shravan Kumar P, Vinay Kumar Awaar, and Praveen Jugge, DSP based voltage source inverter for an application of induction motor control, eISSN: 2267-1242, E3S Web Conf. **184**, 01057 (2020)

11. O. Sandre-Hernandez, P. Ordaz-Oliver and C. Cuvas-Castillo, Sensorless field oriented control of bldc motor based on sliding mode observer, International Conference on Mechatronics, Electronics and Automotive Engineering (ICMEAE) (2019), pp. **119-124**

12. N. Biniakos, V. Iakovakis, Sensored field oriented control of BLDC motor for pico satellite attitude control, International Journal of Innovative Science and Research Technology, **4** (2019)

13. Sattu, Shravani, Vinay Kumar Awaar, and Praveen Jugge, Speed control of robust position sensorless PMBLDC motor by fuzzy controller, In E3S Web of Conferences, vol. **309**, p. 01063. EDP Sciences, (2021)